ELSEVIER

Catalysis Today 50 (1999) 133–140

CATALYSIS TODAY

Kinetics of the selective catalytic reduction of NO with NH_3 over MnO_x/Al_2O_3 catalysts at low temperature

W. Sjoerd Kijlstra, Danny S. Brands, Eduard K. Poels, Alfred Bliek*

Department of Chemical Engineering, University of Amsterdam, Nieuwe Achtergracht 166, 1018 WV Amsterdam, The Netherlands

Abstract

The steady-state kinetics of the selective catalytic reduction of NO with NH_3 have been studied over a 2 wt% Mn/Al_2O_3 catalyst at 423 K using wide concentration ranges for NO, NH_3 and O_2. Rate equations have been derived which are based on a previously elucidated mechanistic model including *parallel* Langmuir–Hinshelwood (LH) and Eley–Rideal (ER) pathways to N_2 production and inhibition by product water. These equations provide significantly better fits of the kinetic data than rate equations based on either LH or ER mechanisms and may be used for further reactor design. © 1999 Elsevier Science B.V. All rights reserved.

Keywords: Selective catalytic reduction; Steady-state kinetics

1. Introduction

Selective catalytic reduction (SCR) of NO with NH_3 is considered as the most proven way to remove NO_x from flue gases emitted by stationary sources. To apply the SCR technique in add-on units, catalysts active at low temperatures (<473 K) are desired, thus avoiding reheating of the stack gases. Alumina supported manganese oxides appeared to be very active catalysts for this reaction in the temperature range 383–573 K [1]. The extent of inhibition by water vapour is limited at space velocities of industrial interest at these low temperatures [2]. Moreover, the selectivity towards N_2 production exceeds 99% for low Mn loadings [3]. Therefore, the attention has been focused on a 2 wt% Mn/Al_2O_3 catalyst. As a result of the favourable catalytic properties, it might be interesting to obtain a kinetic rate expression for this catalyst, based on a mechanistic model, suitable for further reactor design.

Several kinetic studies have been reported in literature, mainly on high temperature SCR catalysts (500–700 K). Depending on the used catalysts, rate equations based on both of Eley–Rideal (ER) mechanism [4,5] and a Langmuir–Hinshelwood (LH) mechanism [6–8] are derived. In several rate equations, inhibition by H_2O was included in the model [4,6–8]. However, based on extensive mechanistic studies using transient techniques, temperature programmed desorption (TPD) and FTIR [9,10], we recently reported *parallel* ER and LH mechanisms for a 2 wt% Mn/Al_2O_3 catalyst, although the major part of the N_2 was formed via the ER route. A preliminary kinetic study [2] resulted in the following power rate:

$$r_{NO} = k^* p_{NO}^{a^*} p_{NH_3}^{b^*} p_{O_2}^{c} \quad (1)$$

*Corresponding author. Tel.: +31-20-525-6479; fax: +31-20-525-5604; e-mail: bliek@chemeng.chem.uva.nl

0920-5861/99/$ – see front matter © 1999 Elsevier Science B.V. All rights reserved.
PII: S0920-5861(98)00470-2

with fitted values of 0.79, −0.04 and 0.51, for *a*, *b* and *c*, respectively. As *a* is significantly smaller than one, a rate equation simply based on an ER mechanism is not able to describe the set of steady-state kinetic data.

In this paper, kinetic equations are derived, based on the previously presented scheme including parallel ER- and LH-mechanisms and inhibition by product H_2O [10], which are able to describe a very broad set of steady-state kinetic data at the low temperature of interest (423 K).

2. Experimental

2.1. Catalyst

The 2 wt% Mn/Al_2O_3 catalyst was prepared by incipient wetness impregnation of a Ketjen CK300 γ-Al_2O_3 support (S_{BET}=192 $m^2\ g^{-1}$, pore volume= 0.5 $cm^3\ g^{-1}$ and particle size=150–250 μm) with an aqueous solution of $(CH_3COO)_2Mn{\cdot}4H_2O$. Subsequently, the catalyst was dried in stagnant air overnight at 383 K, followed by calcination in O_2 at 573 K for 1 h and at 773 K for 3 h. Due to the limited solubility of the precursor, the impregnation was performed in two steps with drying in-between. A more detailed characterisation of this catalyst was reported previously [3,11].

2.2. Gases

0.40 vol% NO/He, 0.40 vol% NH_3/He, O_2 (99.6% purity), and He (99.996%) were used during the flow reactor studies (UCAR). The O_2 was dried before use by molecular sieves (5 A, Janssen Chimica).

2.3. Conditions and procedure

The entire set of kinetic data was measured at 423 K. The partial pressures of NO, NH_3 and O_2 were varied between 11–135 Pa, 12–150 Pa and 0.25–10 kPa (balance He), respectively. The catalysts were fixed in tubular reactors (3.3 mm i.d.), resulting in bed heights of 1.6 cm. Five reactors, loaded with one 80 mg, two 40 mg and two 20 mg catalyst samples, were analysed simultaneously in a set-up described previously [12]. The catalysts samples were diluted with γ-Al_2O_3 to establish equal bed heights. It has been verified that the diluent did not contribute significantly to the NO conversion at the applied temperature. The total flow rate used through each reactor was 50 ml min^{-1}.

Before starting the kinetic measurements the catalyst samples were pretreated in 2 vol% O_2/He at 673 K for 1 h, followed by cooling down to the reaction temperature in the same atmosphere. At this temperature a *standard reaction mixture*, containing 45 Pa NO, 50 Pa NH_3 and 2 kPa O_2, was passed over the reactors for 200 h to establish steady-state conditions. Previously, we reported that such a long stabilisation period is necessary to obtain a constant, equilibrated amount of bidentate nitrates on the catalyst surface [10]. Subsequently, another gas phase composition was chosen within the experimental grid and was passed over the catalysts during 3 h, which appeared to be sufficient to establish a new steady-state. Every 3 h a new gas phase composition was chosen, at random. After having measured 3–4 different grid points, the standard reaction mixture was passed over the reactors for 3 h; the activity was always reproduced within 2% NO conversion under these conditions. By this procedure, the NO conversion was obtained as a function of W/F_{NO} and the partial pressures of NO, NH_3 and O_2. As the detected amounts of N_2O were negligible, the NO conversion is considered as a reliable parameter to express the reaction rate towards N_2.

2.4. Parameter estimation

The calculated NO conversion is obtained from the continuity equation (Eq. (2)) of a plug flow reactor under steady-state conditions:

$$\frac{dX_{NO}}{dW/F_{NO}} = r_{NO}(X_{NO}, p_{NO}, p_{NH_3}, p_{O_2}, k_i \ldots, K_i \ldots) \quad (2)$$

The unknown rate constants k_i and equilibrium constants K_i are estimated from the experimental data using the non-linear least-squares Simplex and Levenberg–Marquardt methods, whereby the sum of least squares of the residual NO conversion (observed minus calculated conversion) was minimised. An integral reactor behaviour was accounted for as the measured NO conversions ranged from 0.03 to 0.70. As a result, Eq. (2) had to be integrated numerically

for each data point within the minimisation procedure to obtain the calculated NO conversion at the reactor exit. This integration was conducted by the use of the Bulirsch–Stoer technique [13].

2.5. Mass and heat transfer limitations

The absence of mass and heat transfer limitations was verified by calculation, based on the highest activities, of the following four dimensionless criteria [14]:

$$(1)\quad \mathrm{Ca} = 0.005 \ll 0.05, \tag{3}$$

$$(2)\quad \beta_e^* \gamma^* \mathrm{Ca} = 0.017 < 0.05, \tag{4}$$

$$(3)\quad \eta^* \phi^2 = 0.024 < 0.15, \tag{5}$$

$$(4)\quad \beta_i^* \gamma^* \eta^* \phi^2 = 10^{-4} \ll 0.05. \tag{6}$$

Criteria (3) and (4) refer to transport from the gas phase to the catalyst particles, criteria (5) and (6) to transport within the catalyst particles. Furthermore, given that the ratios d_t/d_p range from 22 to 31 and L/d_p from 93 to 132 one may assume a flat velocity profile and a negligible axial dispersion [14].

3. Results and discussion

According to the previously reported discussion on the SCR reaction mechanism on a 2 wt% Mn/Al_2O_3 catalyst [10], the following reaction scheme can be formulated for temperatures below 500 K

(a) $O_2 + 2^* \rightleftharpoons 2O\text{–}^*$ $\quad K_1 = k_1/k_{-1}$

(b) $NH_3 + ^* \rightleftharpoons NH_3^*\text{–}$ $\quad K_2 = k_2/k_{-2}$

(c) $NO + O\text{–}^* \rightleftharpoons NO\text{–}O\text{–}^*$ $\quad K_3 = k_3/k_{-3}$

(d) $NO\text{–}O\text{–}^* + O\text{–}^* \rightleftharpoons NO_3\text{–}^* + ^*$ $\quad K_4 = k_4/k_{-4}$

(e) $NH_3\text{–}^* + O^*\text{–} \rightleftharpoons NH_2\text{–}^* + OH\text{–}^*$ $\quad K_5 = k_5/k_{-5}$

(f) $NH_2^*\text{–} + NO \rightarrow N_2 + H_2O + ^*$ $\quad k_6$

(g) $NH_2\text{–}^*\text{–} + NO\text{–}O\text{–}^* \rightarrow N_2 + H_2O + O\text{–}^* + ^*$ $\quad k_7$

(h) $2OH\text{–}^* \rightleftharpoons H_2O + O^*\text{–} + ^*$ $\quad K_8 = k_8/k_{-8}$

In this scheme * represents an adsorption site. It should be mentioned that adsorption of NH_3 and O_2 may take place on one Mn-site which is two fold coordinatively unsaturated. The reaction steps (f) and (g) run in parallel, but the major part of the N_2 is produced via step (f) [10]. As these two steps are assumed to be rate determining while the other steps are considered to be in quasi-equilibrium, the conversion rate of NO towards N_2 can be written as

$$r_{NO} = r(f) + r(g). \tag{7}$$

Because the data were obtained after a stabilisation period of 150 h, during which a stable concentration of bidentate nitrates on the catalyst surface is established, the equilibrium of step (d) in the model was omitted for the derivation of the reaction rate equation. After substitution of the steps (f) and (g) and accounting for the equilibria (a)–(c), (e) and (h) Eq. (7) yields:

$$r_{NO} = \frac{k' * p_{O_2}^{1/4} p_{NO} p_{NH_3}}{\sqrt{p_{H_2O}} A} + \frac{k'' * p_{O_2}^{3/4} p_{NO} p_{NH_3}}{\sqrt{p_{H_2O}^*} A^2} \tag{7b}$$

in which

$$A = 1 + \sqrt{K_1 P_{O_2}} + K_2 p_{NH_3} + K_3 p_{NO} + K_d \sqrt{p_{H_2O}} p_{O_2}^{1/4} + K_e \frac{p_{NH_3}}{\sqrt{p_{H_2O}}} p_{O_2}^{1/4}, \tag{8}$$

$$K_d = \frac{K_1^{1/4}}{\sqrt{K_8}}, \tag{9}$$

$$K_e = K_1^{1/4} K_2 \sqrt{K_8} K_5, \tag{10}$$

$$k' = N_t k_6 K_e, \tag{11}$$

$$k'' = N_t s k_7 \sqrt{K_1} K_3 K_e. \tag{12}$$

This equation has been used to fit the steady-state kinetic data at 423 K. The constants k' and k'' as well as the equilibrium constant K_1, K_2, K_3, K_d and K_e were determined using a Simplex algorithm. The residual analysis of the results is shown in Fig. 1. The residuals should be equally distributed around zero with nearly zero mean, without any trends as a function of the dependent or independent variables. From the presented plots it is clear that there is indeed an equal distribution of residuals, except for some deviation at very low oxygen partial pressures. Hence, based on the residual plot analysis, Eq. (7b) provides a satisfactory fit of the data.

The values of the determined constants are presented in Table 1. The experimental data are given in Appendix A. Moreover, the statistic parameters R^2 and mean-SSR are given in the table. The mean-

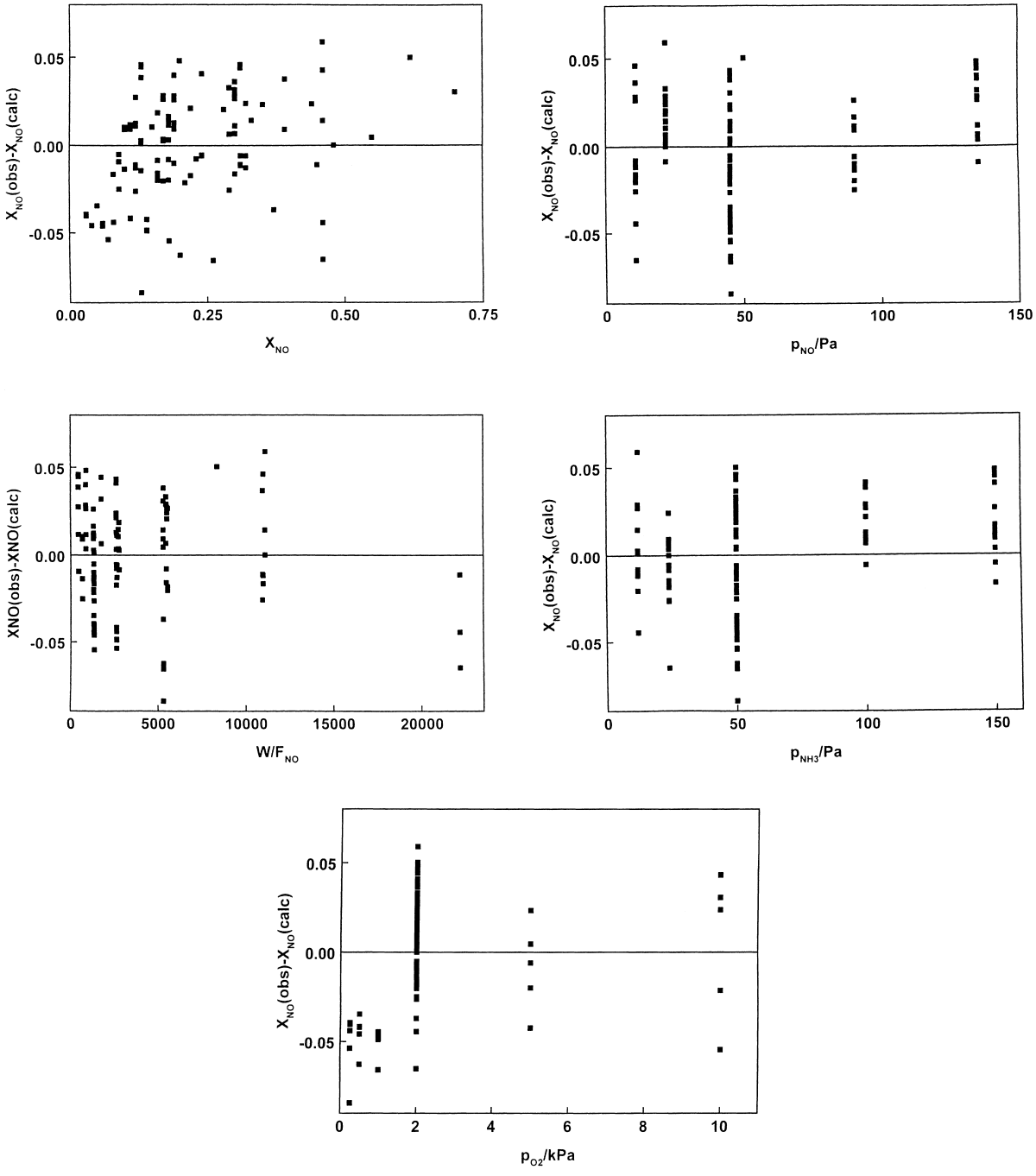

Fig. 1. Residual NO conversion (observed minus calculated NO conversion) as a function of independent and dependent variables: (a) conversion, (b) space time $(W F_{NO}^{-1}/\mathrm{kg\,s\,mol^{-1}})$, (c) p_{NO}/Pa, (d) p_{NH_3}/Pa and (e) p_{O_2}/kPa; Eq. (7b).

Table 1
Parameter estimates with 95% confidence limits according to Eqs. (7b) and (15)

	Eq. (7b)	Eq. (15)
k'	$0.289\ (\pm 0.179)\times 10^{-7}$	$0.168\ (\pm 0.081)\times 10^{-5}$
k''	$0.740\ (\pm 0.411)\times 10^{-8}$	$0.173\ (\pm 0.098)\times 10^{-6}$
K_1	0.807×10^{-9}	
K_2	$0.272\ (\pm 0.192)\times 10^{-1}$	0.128 ± 0.050
K_3	$0.777\ (\pm 0.579)\times 10^{-2}$	$0.137\ (\pm 0.092)\times 10^{-1}$
K_d	0.780×10^{-5}	
K_e	$0.193\pm(0.070)$	
K_8		$0.443\ (\pm 0.296)\times 10^{-1}$
Mean-SSR	0.954×10^{-3}	0.503×10^{-3}
R^2	0.989	0.993

SSR is defined as follows:

$$\text{mean}-\text{SSR} = \frac{\text{SSR(min)}}{\text{df}} \tag{13}$$

in which SSR=sum of squared residuals and df=degrees of freedom (number of data points minus number of estimated parameters). As all data points are accounted for equally, R^2 is defined as

$$\frac{\left|\sum_{i=1}^{n} X_{\text{NO}}(\text{obs})_i^2 - \sum_{i=1}^{n}(X_{\text{NO}}(\text{obs})_i - X_{\text{NO}}(\text{cal})_i)^2\right|}{\sum_{i=1}^{n} X_{\text{NO}}(\text{obs})_i^2}. \tag{14}$$

The value for the mean-SSR is very small, indicative for an appropriate fit of the data. In contrast, the confidence intervals of the rate and equilibrium constants are large, the interval of K_1 and K_d being so large that the accuracy of these constants is very limited.

As a result of the impractically broad confidence limit of K_1, we simplified the proposed model slightly to obtain a less complex rate equation with five parameters to be estimated (instead of seven). Therefore, the equilibrium (a) of the above model was omitted, by assuming a constant excess of oxygen in the flue gas. Moreover, formation of amide species is no longer considered as a separate step, but is included in a concerted step towards N_2-production. As a result, the amide species in steps (f) and (g) was replaced by coordinated NH_3 species. As no hydroxyls are formed in this model, the inhibition by H_2O was represented by modifying equilibrium (h):

(h) $H_2O + {}^* \rightleftharpoons H_2O{-}^*$ $\qquad K_8 = k_8/k_{-8}$

The main characteristic of the model, i.e. a parallel ER and LH route to N_2, is maintained. As a result of these modifications, Eq. (7b) is simplified to

$$r_{\text{NO}} = \frac{(k' * p_{\text{NO}} p_{\text{NH}_3})}{(1 + K_2 p_{\text{NH}_3} + K_3 p_{\text{NO}} + K_8 p_{\text{H}_2\text{O}})} + \frac{(k'' p_{\text{NO}} p_{\text{NH}_3})}{(1 + K_2 p_{\text{NH}_3} + K_3 p_{\text{NO}} + K_8 p_{\text{H}_2\text{O}})^2}, \tag{15}$$

in which

$$k' = k_6^* N_t^* K_2, \tag{16}$$

$$k'' = k_7^* N_t^* s^* K_2^* K_3. \tag{17}$$

Parameter estimation was performed with the same set of data at 423 K; only the data in which the partial pressure of O_2 varies ($p_{O_2 \neq 2.0\,\text{kPa}}$) were omitted. This equation provides well defined constants and even a better fitting of the data (see Table 1), with a smaller value of the mean-SSR and a value of R^2 closer to unity. The residual plots (Fig. 2) show no tendencies at all and the absolute variation around zero is smaller than observed for the residuals resulting from Eq. (7b). Hence, this equation shows that a model in which an ER and a LH mechanism run in parallel can nicely describe a wide range of kinetic data. This is a remarkable result as many mechanistic studies on the SCR reaction on other catalysts do not address the possibility of parallel pathways. Recently, competition of both mechanisms was proposed for CuO/Al_2O_3 catalysts [15].

Finally, the entire dataset has been fit with two 'classical' models that are based on mechanistic insights that are comparable to our reported conclusions in [10], *except* for the fact that only one pathway, either LH or ER, to N_2 production is included. First, the model VI reported by Odenbrand et al. [5], assuming equilibrated concentrations of NH_2 and O_2 on the catalyst surface, followed by reaction with gas phase NO, was used to fit the data. Irrespective of the initial values of the constants, trends in the residual plots were observed and the value for the mean-SSR was two orders of magnitude higher than the values reported in Table 1. A second rate equation, based on a LH mechanism which nicely describes the kinetic data for a (high loaded) Mn_2O_3–WO_3/Al_2O_3 catalysts, was reported by Kapteijn et al. (Eq. (17), [16]). For the present dataset on a 2 wt% Mn/Al_2O_3 catalyst, this equation gives a fit with nice residual plots and mean-

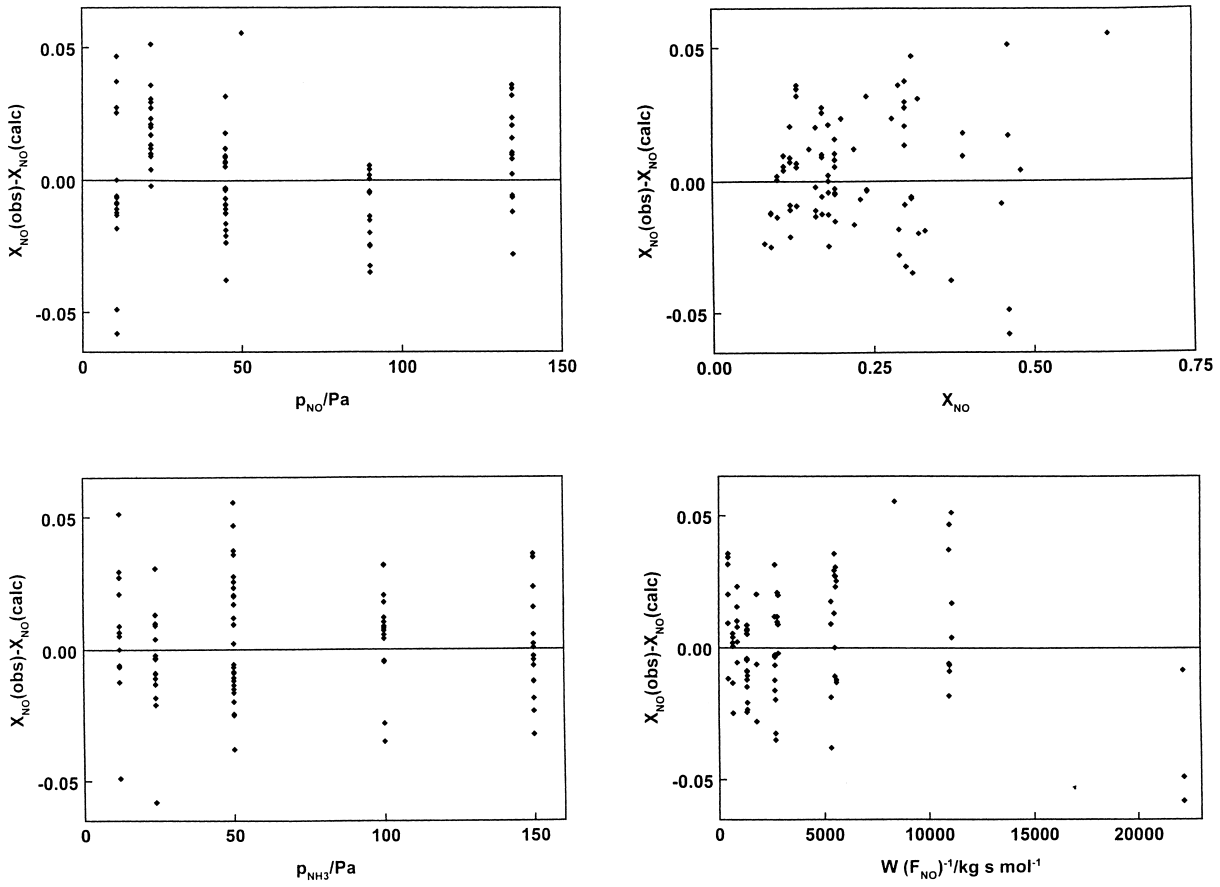

Fig. 2. Residual NO conversion (observed minus calculated NO conversion) as a function of independent and dependent variables: (a) conversion, (b) space time ($W F_{NO}^{-1}$/kg s mol^{-1}), (c) p_{NO}/Pa and (d) p_{NH_3}/Pa; Eq. (15).

SSR, but three of the five constants do not significantly differ from zero, reducing this equation to an ordinary power rate law.

4. Conclusions

On low loaded Mn/Al_2O_3 SCR catalysts both the Langmuir–Hinshelwood and an Eley–Rideal mechanism are operative. Therefore, rate equations reported so far on other SCR catalysts based on one of these routes are not suitable to describe the wide range of steady-state kinetic data at 423 K, measured in this paper. A reaction rate equation has been derived including parallel N_2 production by both pathways and inhibition by product water. This equation is able to fit the entire kinetic dataset without any trends and may serve for further reactor design.

5. Nomenclature

a	reaction order in partial pressure NO (dimensionless)
A	constant; summation of all adsorption terms (dimensionless)
b	reaction order in partial pressure NH_3 (dimensionless)
c	reaction order in partial pressure O_2 (dimensionless)
Ca	Carberry number [14] (dimensionless)
d_t	diameter of reactor tube (m)

d_p	diameter of catalyst particle (m)
F_{NO}	molar flow rate of NO (mol s^{-1})
k_i, k_{-i}	rate constant of process i (1)
L	reactor length (m)
N_t	total concentrations of active sites (mol kg^{-1})
p_i	partial pressure of component i (Pa)
r_i	rate of process i (mol kg^{-1} s^{-1})
s	concentration of neighbouring sites (mol kg^{-1})
W	catalyst weight (kg)
β_i	Prater number [14] (dimensionless)
β_e	external Prater number [14] (dimensionless)
γ	dimensionless activation energy (dimensionless)
η	effectiveness factor of the catalyst [14] (dimensionless)
φ	Thiele modulus (dimensionless)
(1)	the dimension depends on the elementary process, which is used.

Appendix A

Experimental data

X_{NO}	W/F_{NO}	p_{NO} (Pa)	p_{NH3} (Pa)	p_{O2} (kPa)
0.13	5320	45	50	0.25
0.08	2633.3	45	50	0.25
0.07	2627.8	45	50	0.25
0.03	1340	45	50	0.25
0.03	1320	45	50	0.25
0.2	5320	45	50	0.5
0.11	2633.3	45	50	0.5
0.11	2627.8	45	50	0.5
0.04	1340	45	50	0.5
0.05	1320	45	50	0.5
0.26	5320	45	50	1
0.14	2633.3	45	50	1
0.14	2627.8	45	50	1
0.06	1340	45	50	1
0.06	1320	45	50	1
0.37	5320	45	50	2
0.23	2633.3	45	50	2
0.22	2627.8	45	50	2
0.12	1340	45	50	2

Appendix A (*Continued*)

X_{NO}	W/F_{NO}	p_{NO} (Pa)	p_{NH3} (Pa)	p_{O2} (kPa)
0.12	1320	45	50	2
0.55	5320	45	50	5
0.35	2633.3	45	50	5
0.32	2627.8	45	50	5
0.14	1340	45	50	5
0.16	1320	45	50	5
0.7	5320	45	50	10
0.46	2633.3	45	50	10
0.44	2627.8	45	50	10
0.18	1340	45	50	10
0.21	1320	45	50	10
0.46	22167.8	10.8	12	2
0.31	10974.4	10.8	12	2
0.31	10946.7	10.8	12	2
0.17	5583.3	10.8	12	2
0.18	5501.1	10.8	12	2
0.46	22167.8	10.8	24	2
0.3	10974.4	10.8	24	2
0.29	10946.7	10.8	24	2
0.16	5583.3	10.8	24	2
0.16	5501.1	10.8	24	2
0.45	22167.8	10.8	50	2
0.31	10974.4	10.8	50	2
0.3	10946.7	10.8	50	2
0.17	5583.3	10.8	50	2
0.17	5501.1	10.8	50	2
0.46	11083.3	21.6	12	2
0.3	5536.7	21.6	12	2
0.3	5473.3	21.6	12	2
0.17	2791.1	21.6	12	2
0.18	2750	21.6	12	2
0.48	11083.3	21.6	24	2
0.32	5536.7	21.6	24	2
0.3	5473.3	21.6	24	2
0.16	2791.1	21.6	24	2
0.17	2750	21.6	24	2
0.46	11083.3	21.6	50	2
0.28	5536.7	21.6	50	2
0.29	5473.3	21.6	50	2
0.16	2791.1	21.6	50	2
0.15	2750	21.6	50	2
0.13	1340	45	12	2
0.13	1320	45	12	2
0.39	5320	45	24	2
0.24	2633.3	45	24	2

Appendix A (*Continued*)

X_{NO}	W/F_{NO}	p_{NO} (Pa)	p_{NH3} (Pa)	p_{O2} (kPa)
0.24	2627.8	45	24	2
0.12	1340	45	24	2
0.13	1320	45	24	2
0.37	5320	45	50	2
0.23	2633.3	45	50	2
0.22	2627.8	45	50	2
0.12	1340	45	50	2
0.12	1320	45	50	2
0.39	5320	45	100	2
0.24	2633.3	45	100	2
0.22	2627.8	45	100	2
0.12	1340	45	100	2
0.12	1320	45	100	2
0.33	5320	45	150	2
0.19	2633.3	45	150	2
0.18	2627.8	45	150	2
0.08	1340	45	150	2
0.09	1320	45	150	2
0.32	2660.1	90	50	2
0.19	1316.9	90	50	2
0.18	1313.7	90	50	2
0.09	669.9	90	50	2
0.1	660.1	90	50	2
0.31	2660.1	90	100	2
0.19	1316.9	90	100	2
0.19	1313.7	90	100	2
0.11	669.9	90	100	2
0.11	660.1	90	100	2
0.3	2660.1	90	150	2
0.19	1316.9	90	150	2
0.18	1313.7	90	150	2
0.1	669.9	90	150	2
0.1	660.1	90	150	2
0.3	1773.3	135	50	2
0.18	877.9	135	50	2
0.17	864.7	135	50	2
0.09	446.7	135	50	2
0.11	440.1	135	50	2
0.29	1773.3	135	100	2
0.19	877.9	135	100	2

Appendix A (*Continued*)

X_{NO}	W/F_{NO}	p_{NO} (Pa)	p_{NH3} (Pa)	p_{O2} (kPa)
0.19	864.7	135	100	2
0.12	446.7	135	100	2
0.13	440.1	135	100	2
0.31	1773.3	135	150	2
0.2	877.9	135	150	2
0.19	864.7	135	150	2
0.13	446.7	135	150	2
0.13	440.1	135	150	2

References

[1] L. Singoredjo, R. Korver, F. Kapteijn, J.A. Moulijn, Appl. Catal. B 1 (1992) 297.
[2] W.S. Kijlstra, J.C.M.L. Daamen, J.M. van de Graaf, B. van der Linden, E.K. Poels, A. Bliek, Appl. Catal. B 7 (1996) 337.
[3] W.S. Kijlstra, E.K. Poels, A. Bliek, B.M. Weckhuysen, R.A. Schoonheydt, J. Phys. Chem. B 101 (1997) 309.
[4] J.A. Dumesic, N.-Y. Topsøe, H. Topsøe, Y. Chen, T. Slabiak, J. Catal. 163 (1996) 409.
[5] C.U.I. Odenbrand, A. Bahamonde, P. Avilla, J. Blanco, Appl. Catal. B 5 (1994) 117.
[6] H.-G. Lintz, T. Turek, Appl. Catal. A 85 (1992) 13.
[7] R.J. Willey, J.W. Eldridge, J.R. Kittrell, Ind. Eng. Chem. Prod. Res. Dev. 24 (1985) 226.
[8] M. Turco, L. Lisi, R. Pirone, P. Ciambelli, Appl. Catal. B 3 (1994) 133.
[9] W.S. Kijlstra, D.S. Brands, E.K. Poels, A. Bliek, J. Catal. 171 (1997) 208.
[10] W.S. Kijlstra, D.S. Brands, H.I. Smit, E.K. Poels, A. Bliek, J. Catal. 171 (1997) 219.
[11] F. Kapteijn, A.D. van Langeveld, J.A. Moulijn, A. Andreini, M.A. Vuurman, A.M. Turek, J.-M. Jehng, I.E. Wachs, J. Catal. 150 (1994) 94.
[12] L. Singoredjo, M. Slagt, J. van Wees, F. Kapteijn, J.A. Moulijn, Catal. Today 7 (1990) 157.
[13] W.H. Press, B.P. Flannery, S.A. Teukolsky, W.T. Vetterling, Numerical Recipes, Cambridge University Press, Oxford, 1989.
[14] J.A. Moulijn, A. Tarfaoui, F. Kapteijn, Catal. Today 11 (1991) 1.
[15] G. Centi, S. Perathoner, J. Catal. 152 (1995) 93.
[16] F. Kapteijn, L. Singoredjo, N.J.J. Dekker, J.A. Moulijn, Ind. Eng. Chem. Res. 32 (1993) 445.